ELSEVIER

International Journal of Mass Spectrometry 195/196 (2000) 639–652

International Journal of Mass Spectrometry

Fundamental factors controlling the exchange of multidentate ligands: displacement of 12-crown-4 and triglyme from complexes with divalent alkaline earth cations

Nanzhu Shen[1], R. Marshall Pope[2], David V. Dearden*

Department of Chemistry and Biochemistry, C100 Benson Science Building, Brigham Young University, Provo, UT 84602-5700, USA

Received 6 August 1999; accepted 3 September 1999

Abstract

In an effort to shed light on the factors that influence the recognition of alkaline earth cations in natural systems, we have studied intrinsic recognition of these cations by well-ordered synthetic ionophores such as crown ethers (12-crown-4 [C4] and 18-crown-6 [C6]) as well as the acyclic analog of C4, triglyme (TG), in the gas phase. We have employed electrospray ionization (ESI) to generate gas phase crown and glyme alkaline earth complexes, and have used Fourier transform ion cyclotron resonance mass spectrometry to measure rate constants for displacement of the original ligands by C6. ESI of mixtures of C4 and TG with alkaline earths primarily produces sandwich complexes of the doubly charged cations, $(C4)_2M^{2+}$, $(C4)(TG)M^{2+}$, and $(TG)_2M^{2+}$. We find that the ligand exchange reactions are generally very efficient, with rates approaching or exceeding the Langevin collision rate in most cases. Trends in rates as metal size varies can be understood in terms of the degree of encapsulation of the metal by the ligands when the coordination shell is partially filled (smaller metals are more thoroughly encapsulated and tend to react more slowly) and in terms of the polarizing power of the metal cation when the metals are either "bare" or completely coordinated (smaller metals have greater charge density and tend to react more rapidly). Efficiencies for most of the reactions studied fall off in the order $Mg^{2+} > Ca^{2+} > Sr^{2+} > Ba^{2+}$, consistent with decreasing charge density as the cation radius increases. Interestingly, TG is displaced more efficiently than C4 by C6, despite the fact that the total binding energy of the glyme is greater than that of the crown. This is consistent with a mechanism wherein the rate-limiting step involves breaking $O–M^{2+}$ electrostatic bonds, and where the bonds to the oxygens of TG can be broken one at a time, whereas the more rigid ring structure of C4 requires concerted breaking of multiple bonds. Molecular dynamics simulations of this process for complexes where $M^{2+} = Ca^{2+}$ give support to this interpretation: in all observed dissociation events, TG oxygens were removed from the metal one at a time, whereas displacement of C4 oxygens occurred in pairs. (Int J Mass Spectrom 195/196 (2000) 639–652) © 2000 Elsevier Science B.V.

Keywords: Ligand exchange; Crown ether; Alkaline earth; Fourier transform ion cyclotron resonance; Molecular dynamics

1. Introduction

The alkaline earth metals and their compounds play significant roles in biological systems, organometallic chemistry, radioactive metal-based therapeutics, and nuclear energy research [1–4]. The important

* Corresponding author. E-mail: david_dearden@byu.edu

[1] Present address: Novartis Crop Protection, Greensboro, NC.

[2] Present address: University of North Carolina School of Medicine, Chapel Hill, NC.

Dedicated to the memory of Professor Bob Squires.

PII S1387-3806(99)00199-2

role of M^{2+}, especially Mg^{2+} and Ca^{2+}, as messengers in a wide variety of cellular processes [4] makes the study of M^{2+} ionophores important. For example, it has been reported that the diversity of calcium-mediated biochemical processes arises from the direct binding of calcium ion to selective sites on the surface of proteins where oxygen comprises the great majority of metal-binding donor atoms [5–7]. Frequently, simple model ligands such as crown ethers have been used to probe the selective binding of alkaline earths in solution [8–11] and the solid state [12–15]. These studies are attractive because the synthetic ligands are far simpler than the proteins they mimic, yet still exhibit high degrees of selectivity, making it possible to isolate the fundamental factors that lead to selective binding. In addition, with simple synthetic ligands it is straightforward to probe such issues as the effects of donor atom number and/or type, substituents, or anions on binding constants and selectivity.

The complexes of Mg^{2+}, Ca^{2+}, and Sr^{2+} with NH_3 and H_2O have been characterized using computational methods [16,17]. An ab initio study of the complexes of 18-crown-6 (C6) with the alkaline earths [18] found that in the gas phase Mg^{2+}, Ca^{2+}, Sr^{2+}, and Ba^{2+} all fit easily in the cavity of the ligand, and that all are strongly bound with ligand binding energies decreasing monotonically with increasing metal size. This contrasts with the pattern of ligand binding constants observed in most solvents, which show selectivity for Ba^{2+} [8], but inclusion of 5 or 6 water molecules in the calculation recovered the qualitative order of solution selectivity.

The gas phase reactions of a few monopositive and ligated, singly charged alkaline earths with a number of small ligands have been studied experimentally [19–21]. It has been shown that alkaline earth cations have a natural affinity in the gas phase for oxygen donors, in contrast to transition metal cations, which have a greater tendency to prefer nitrogen donors [22]. The gas phase complexes of monopositive alkaline earths with polyethers have also been examined [23]. The advent of electrospray ionization has made generation of complexes of doubly charged alkaline earths relatively straightforward. For example, the interaction of Mg^{2+} and Ca^{2+} with cell surface carbohydrates [24] has been studied using mass spectrometry.

Relatively little is known about the detailed mechanism of ligand exchange in systems such as these. In solution it is difficult to observe the process directly in real time. Chromophores suitable for spectroscopic studies are generally not available. Further, ligand exchange is believed to be complex, involving displacement of solvent molecules from both the metal and the ligands, and it is believed to take place on a very short time scale. In the gas phase, mass spectrometry offers a convenient means of observation, the complexity of solvation is removed, and reactions can easily be slowed down by decreasing the pressure, so the gas phase is an arena where exchanges can be examined directly and in detail.

In this article, we focus on the gas phase ligand displacement reactions of divalent alkaline earths bound to the simplest crown ether, 12-crown-4 (C4), and/or its acyclic analog, triglyme (TG), with C6. These studies are designed to yield information about the dynamics of multidentate ligand substitution reactions, in the absence of the complicating effects of solvation. We find that the TG complexes undergo ligand displacement by C6 more easily than the C4 complexes, and that the trends in rate constants as the metals are varied can be explained in terms of the degree of encapsulation of the metal by the ligands and the polarizing capabilities of the metals. The experimental studies are complemented by molecular dynamics simulations of the displacement process, that provide insight into the detailed mechanism and suggest an explanation for the differences in the TG and C4 rates.

2. Experimental

All experiments were carried out in a Fourier transform ion cyclotron resonance mass spectrometer (model APEX 47e; Bruker Daltonics; Billerica, MA), equipped with an ion source external to a 4.7 tesla superconducting magnet. A commercial electrospray source with a hexapole ion guide (model 10413; Analytica; Branford, MA) was adapted for micro-

spray by replacing the 34-gauge stainless steel spray capillary with a 50 μm i.d. (inner diameter) glass capillary having a tapered tip (made by grinding with diamond grit) and exchanging the manufacturer's glass capillary vacuum interface with a heated, type 316 stainless steel desolvating tube [0.0625 in. o.d. (outer diameter) × 0.020 in. i.d.]. A microscope (Nippon Kogaku, Japan) with about 100× magnifying power was set up near the spray capillary to monitor spray conditions. Stored waveform inverse Fourier transform (SWIFT) [25,26] was used to isolate selected ions.

12-Crown-4 (C4), 18-crown-6 (C6), triglyme (TG, the acyclic analogue of C4), and alkaline earth metal chlorides (MCl_2, M = Mg, Ca, Sr, and Ba) were purchased from Aldrich (Milwaukee, WI) and used without further purification. Two "cocktail" solutions with MCl_2 and ligands C4 and TG, respectively, were prepared in 50:50 methanol:water as electrospray solutions. The concentrations of metals and ligands in these solutions were 1.2 mM for each metal and 2.5 mM for each ligand. C6 was introduced into the ion cyclotron resonance (ICR) analyzer cell through a gate valve where a solid probe was inserted. The pressure of the neutral was monitored by a magnetically shielded cold cathode gauge (model IKR 050, Balzers), corrected using the method of Bartmess and Georgiadis [27] with polarizabilities calculated using the method of Miller and co-worker [28,29]. The absolute values of the pressures were also estimated based on the rate of exothermic proton transfer from sprayed protonated C4 to C6, and found to be in reasonable agreement with the corrected cold cathode gauge readings.

Ligand exchange reactions between "sandwich" complexes $(L)_2M^{2+}$ (L = C4 and/or TG) and C6 were studied. Double resonance experiments [30] on products formed during the ligand exchange reaction between $(C4)_2Ca^{2+}$ and C6 were also performed to elucidate the reaction mechanisms. Rate experiments were typically conducted for several systems simultaneously, in order to eliminate relative errors in the rate constants arising from pressure fluctuations of the neutral reagent. Rate constants were extracted from the data using a macro developed for Microsoft Excel, "kinfit," which numerically solves a coupled system of differential equations and fits the experimental data to the numerical solution with the rate constants as free parameters.

Molecular modeling was done using HYPERCHEM version 3.0 (Autodesk Inc.; Sausalito, CA). Structures of the 1:1 and 2:1 complexes of C4, C6, and TG with calcium were obtained using the AMBER force field [31] implemented in HyperChem. Semiempirical AM1 single-point calculations were used to determine partial charges on the atoms of the neutral ligands. Polarization of the ligands induced by the metal was estimated using mixed mode procedures, as described previously [32]. Molecular dynamics simulations of collisions between C6 and the C4 and TG complexes of Ca^{2+} were carried out, again with the HyperChem version of AMBER. Simulations were run at constant total energy with a simulation temperature of 300 K; the simulation period was more than 200 ps. In particular, distances between Ca^{2+} and the O atoms of the ligands were monitored as a function of simulation time.

Additional molecular modeling and conformational searching was carried out on $(C4)_2Ca^{2+}$, $(TG)_2Ca^{2+}$, $(C4)(C6)Ca^{2+}$, and $(TG)(C6)Ca^{2+}$ using the Merck Molecular Force Field (MMFF94) [33] incorporated in the Spartan modeling package, version 5.1.1 (Wavefunction, Inc.; Irvine, CA). The Spartan Monte Carlo algorithm was used to examine the structures and strain energies of 5184 conformations of $(C4)_2Ca^{2+}$, 2916 conformations of $(TG)_2Ca^{2+}$, 8100 conformations of $(C4)(C6)Ca^{2+}$, and 6561 conformations of $(TG)(C6)Ca^{2+}$.

3. Results

3.1. Kinetic measurements

Ion intensities during the ligand exchange reactions of $(C4)_2Ca^{2+}$, $(C4)(TG)Ca^{2+}$, and $(TG)_2Ca^{2+}$ with C6 are shown in Fig. 1, along with curves derived from fitting the data. Fits are to the solution to the coupled set of differential equations arising from the set of reactions shown in Table 1, which compiles the resulting rate constants and efficiencies relative to

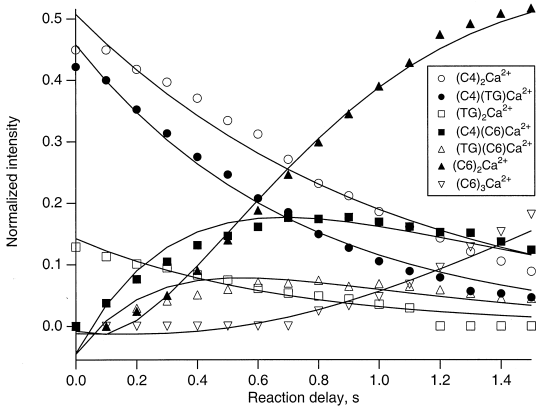

Fig. 1. Normalized intensities of $(C4)_2Ca^{2+}$, $(C4)(TG)Ca^{2+}$, and $(TG)_2Ca^{2+}$ and their reaction products with C6 as a function of reaction time. The pressure of C6 was 2.8×10^{-8} mbar. Solid curves are from fits to the numerical solution of a system of coupled differential equations describing the reaction kinetics.

the Langevin collision rate [34]. The reported errors are standard errors arising from the fit and from averaging replicate measurements.

All of the reactions are fast, with rates 30% of the collision rate or higher; several are faster than the Langevin collision rate. The latter is not surprising in view of possible errors in the absolute pressure measurements; these errors would be directly reflected in the absolute values of the measured rate constants, which are used to calculate the reaction efficiencies. In addition, Langevin theory has a known propensity to underestimate true collision rates [35], especially for polar neutrals such as crown ethers. Although average dipole orientation (ADO) theory [36] would probably do a better job of calculating collision rates, it is difficult to apply here because the required dipole moments of the crowns are conformation dependent and the conformations during collision are unknown. Hence, we use the less accurate but more straightforward Langevin approach. In any event, the relative values for the rate constants and reaction efficiencies, upon which our discussion is based, should be accurate, with relative errors dependent on the standard errors reported.

The least efficient reaction, at 30% of k_{Langevin}, is the terminal reaction of the series, condensation of C6 on $(C6)_2Ca^{2+}$ to form $(C6)_3Ca^{2+}$. This is consistent with expectations for such a complexation reaction, where rates are most likely limited by collisional or radiative stabilization processes.

The most efficient reactions are the displacement of TG from the $(TG)(C6)Ca^{2+}$ complex by C6 and the corresponding displacement of C4 from $(C4)(C6)Ca^{2+}$. Displacement of TG is consistently more efficient than displacement of C4, except in the case of the mixed $(C4)(TG)Ca^{2+}$ complex, where the two reactions occur with essentially the same efficiency.

Results from a separate, similar set of experiments involving displacement by C6 of C4 and/or TG from complexes of Mg^{2+}, Ca^{2+}, Sr^{2+}, and Ba^{2+} are compiled in Fig. 2 and Table 2. Absolute agreement with the Ca^{2+} results of Table 1 is not perfect,

Table 1
Kinetics for reactions of Ca^{2+} complexes with C6[a]

Reaction	Rate constant[b]	Efficiency[c]
$(C4)_2Ca^{2+} + C6 \rightarrow (C4)(C6)Ca^{2+} + C4$	1.35 ± 0.02	0.71 ± 0.01
$(C4)(TG)Ca^{2+} + C6 \rightarrow (C4)(C6)Ca^{2+} + TG$	0.99 ± 0.03	0.52 ± 0.01
$(C4)(TG)Ca^{2+} + C6 \rightarrow (TG)(C6)Ca^{2+} + C4$	0.92 ± 0.03	0.49 ± 0.02
$(TG)_2Ca^{2+} + C6 \rightarrow (TG)(C6)Ca^{2+} + TG$	1.80 ± 0.07	0.95 ± 0.04
$(C4)(C6)Ca^{2+} + C6 \rightarrow (C6)_2Ca^{2+} + C4$	2.95 ± 0.02	1.62 ± 0.01
$(TG)(C6)Ca^{2+} + C6 \rightarrow (C6)_2Ca^{2+} + TG$	4.17 ± 0.04	2.29 ± 0.02
$(C6)_2Ca^{2+} + C6 \rightarrow (C6)_3Ca^{2+}$	0.53 ± 0.01	0.30 ± 0.01

[a] Measurements made simultaneously for the entire set of reactions to minimize error from C6 pressure fluctuations and allow accurate comparison of rate constants. All reported errors are standard errors from the fitting procedure used to determine the rate constants and from averaging replicate determinations.

[b] $\times 10^9$ cm^3 molecule^{-1} s^{-1}.

[c] Relative to Langevin collision rate.

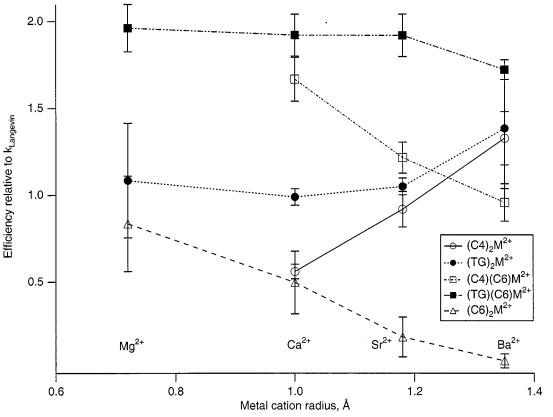

Fig. 2. Efficiencies (relative to Langevin collision rate) for reactions of alkaline earth complexes of C4 and TG with C6. Error bars represent standard error from fitting the data and averaging over replicate data sets. The complexes $(C4)_2M^{2+}$ and $(C4)(C6)M^{2+}$, M = Mg, were not observed.

because the experiments were performed on different days under different pressure conditions, but the relative trends are the same in both data sets, yielding excellent qualitative agreement.

The efficiencies of the displacement of L from $(L)_2M^{2+}$ (L = TG or C4) increase with increasing alkali cation radius. The efficiency is always greater for L = TG than for L = C4, but the difference between the two ligands decreases with increasing metal radius. For the $(L)(C6)M^{2+}$ complexes, L = C4 or TG, the efficiencies decrease with increasing metal radius, and again the trends are stronger for L = C4 than for L = TG. As was noted above for M = Ca, the condensation reactions of $(C6)_2M^{2+}$ are the least efficient for each of the alkali metals, with efficiency decreasing as the metals become larger.

3.2. Molecular dynamics simulations

The results of 200 ps molecular dynamics simulations of the interaction of C6 with $(C4)_2Ca^{2+}$ and $(TG)_2Ca^{2+}$ are depicted in Figs. 3 and 4, respectively, as parametric plots. In these plots, the various Ca^{2+}–O distances for the O atoms of one of the ligands are plotted against each other as simulation time varies. The purpose of this format is to examine correlations in the motions of the O atoms. Population of areas of the graph parallel to either the *x* or *y* axis indicates motion of one of the O atoms with respect to the metal without corresponding motion by the other O atom; population of the diagonal in these plots indicates correlation between the two Ca^{2+}–O distances such that increases or decreases in the Ca^{2+}–O distances occur in a concerted fashion.

Examination of Fig. 3, for displacement of C4 from $(C4)_2Ca^{2+}$, indicates uncorrelated motion for all the Ca^{2+}–O pairs except those involving the adjacent O3, O4 pair; dissociation of these two O atoms occurs together, in a concerted fashion. In Fig. 4, showing the displacement of TG from $(TG)_2Ca^{2+}$, on the other hand, the diagonal regions of the graphs are not populated except for a few points at very large amplitudes. This suggests that although all the O atoms of TG achieve large separations from the metal,

Table 2
Efficiencies for reactions of alkaline earth complexes with C6[a]

Reaction	Efficiency[b]			
	Mg^{2+}	Ca^{2+}	Sr^{2+}	Ba^{2+}
$(C4)_2M^{2+}$ + C6 → $(C4)(C6)M^{2+}$ + C4	—[c]	0.56 ± 0.04	0.92 ± 0.10	1.32 ± 0.15
$(TG)_2M^{2+}$ + C6 → $(TG)(C6)M^{2+}$ + TG	1.08 ± 0.33	0.99 ± 0.05	1.05 ± 0.05	1.38 ± 0.35
$(C4)(C6)M^{2+}$ + C6 → $(C6)_2M^{2+}$ + C4	—[c]	1.66 ± 0.13	1.21 ± 0.09	0.95 ± 0.11
$(TG)(C6)M^{2+}$ + C6 → $(C6)_2M^{2+}$ + TG	1.96 ± 0.14	1.92 ± 0.12	1.92 ± 0.12	1.72 ± 0.06
$(C6)_2M^{2+}$ + C6 → $(C6)_3M^{2+}$	0.84 ± 0.27	0.50 ± 0.18	0.18 ± 0.11	0.05 ± 0.04

[a] Measurements made simultaneously with Ca^{2+} and each of the other alkaline earths, to minimize error from C6 pressure fluctuations and allow accurate comparison of different metals. All reported errors are standard errors from the fitting procedure used to determine the rate constants and from averaging replicate determinations.

[b] Relative to Langevin collision rate.

[c] Not observed.

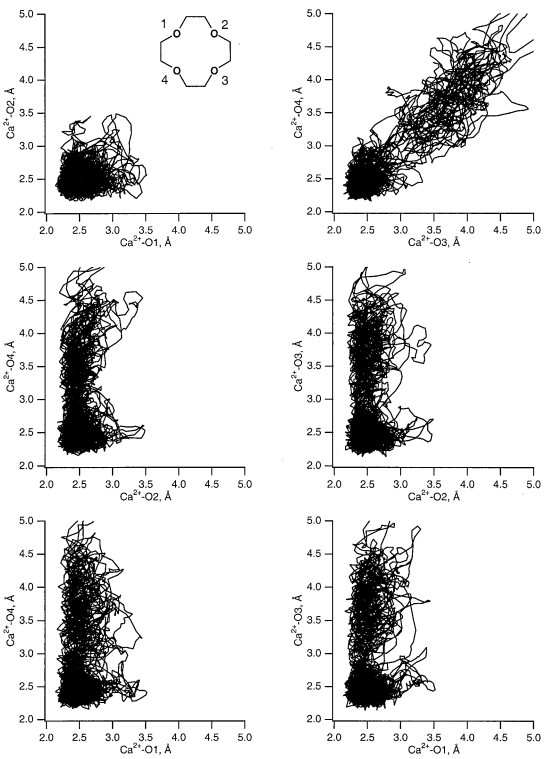

Fig. 3. Parametric plots of distances between Ca^{2+} and the O atoms of one of the C4 ligands during molecular dynamics simulation of collisions between $(C4)_2Ca^{2+}$ and C6. The numbering scheme for the crown O atoms is shown in the inset in the upper left frame. Separations greater than 5 Å are not shown. O3 and O4 dissociated from the metal during the simulation, whereas O1 and O2 remained attached.

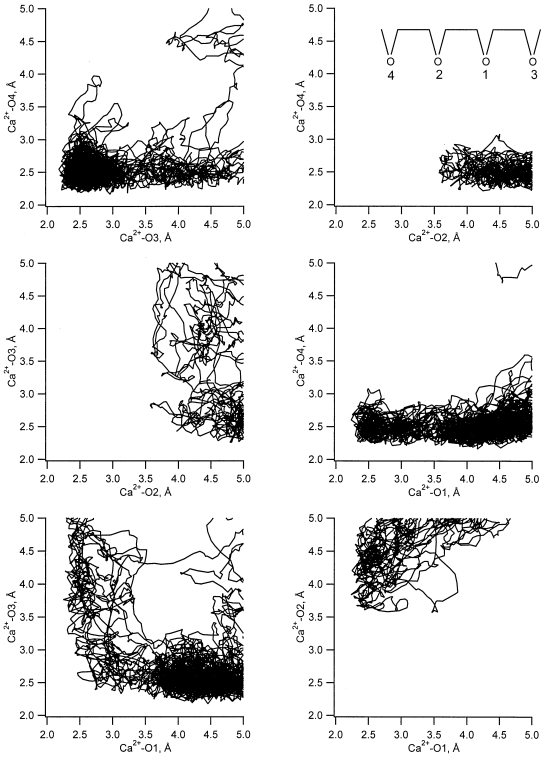

Fig. 4. Parametric plots of distances between Ca^{2+} and the O atoms of one of the TG ligands during molecular dynamics simulation of collisions between $(TG)_2Ca^{2+}$ and C6. The numbering scheme for the triglyme O atoms is shown in the inset in the upper right frame. Separations greater than 5 Å are not shown. All of the O atoms moved to large separations from Ca^{2+} during the simulation, indicating large amplitude motion and at least temporary dissociation from the metal center.

each O moves, to first order, independently of the others (of course at very large scale separations, all the metal–O distances are correlated because all the O atoms are in the same ligand!).

3.3. Conformational searches

The structures of the minimum-energy conformers of $(C4)_2Ca^{2+}$ and $(TG)_2Ca^{2+}$ located after Monte Carlo conformational searching are depicted in Fig. 5. The lowest conformer found for $(C4)_2Ca^{2+}$ is "sandwichlike." It has an eightfold rotational symmetry axis running through the centroids of both C4 ligands and the metal center. The donor O atoms of the two ligands are staggered 45° apart, and the distance from the metal center to the plane of the O atoms in either ligand is 1.5891 Å. Each of the Ca^{2+}–O distances is 2.4806 Å. Another very similar conformer lies only 0.23 kJ mol^{-1} higher in energy, whereas all other located conformers have strain energies more than 13 kJ mol^{-1} higher.

The minimum energy conformer for $(TG)_2Ca^{2+}$ has symmetry that is approximately S_2; the ligands are arranged like the seams of a baseball, such that the donor oxygens of a given ligand are roughly coplanar and the planes of the two ligands are orthogonal. The Ca^{2+} atom is nearly coplanar with each of the donor planes (0.0077 Å from one of the donor planes, and 0.0080 Å from the other). The Ca^{2+}–O distances

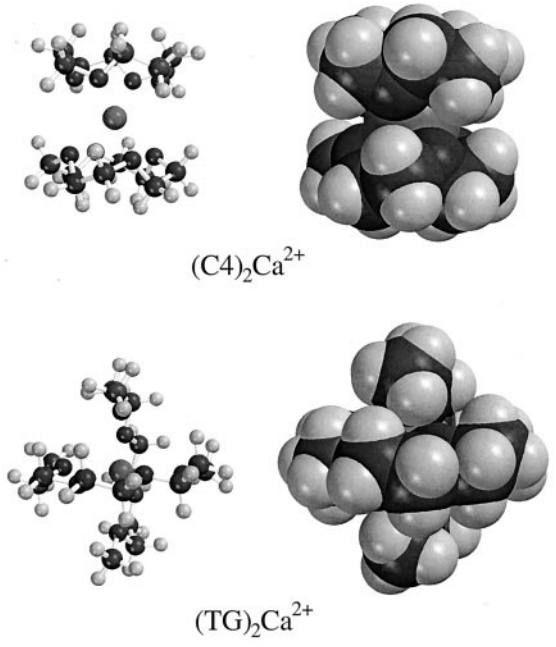

Fig. 5. Ball-and-stick and space-filling models of the lowest energy conformers of $(C4)_2Ca^{2+}$ and $(TG)_2Ca^{2+}$ obtained through Monte Carlo conformational searching using the MMFF94 force field.

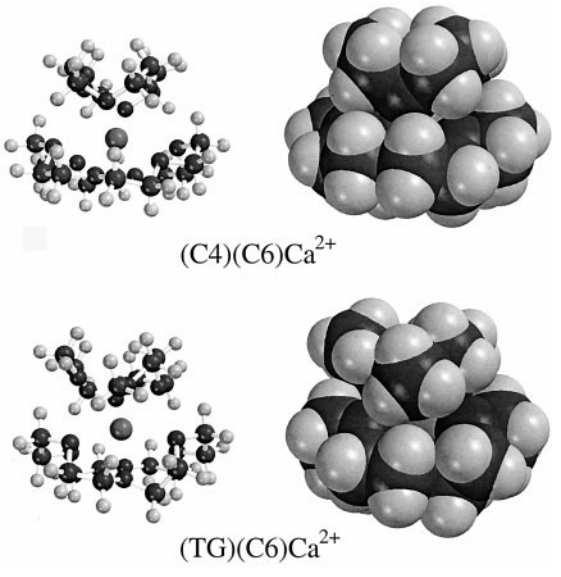

Fig. 6. Ball-and-stick and space-filling models of the lowest energy conformers of $(C4)(C6)Ca^{2+}$ and $(TG)(C6)Ca^{2+}$ obtained through Monte Carlo conformational searching using the MMFF94 force field.

average a little greater than in the $(C4)_2Ca^{2+}$ complex: 2.536 ± 0.012 Å. Many similar, low-lying conformers were found, but the first that has a geometry similar to that of the $(C4)_2Ca^{2+}$ complex (with the two ligands forming pseudo-rings, one above and one below the metal, in sandwich fashion) is 17.8 kJ mol^{-1} higher in energy than the minimum energy conformer.

Structures for the lowest energy conformers located by Monte Carlo searching on $(C4)(C6)Ca^{2+}$ and $(TG)(C6)Ca^{2+}$ are shown in Fig. 6. The lowest energy conformers of both complexes are sandwichlike, but in both cases the metal is displaced toward the C6 ligand and away from the smaller ligand. For instance, considering the ten lowest energy conformers of $(C4)(C6)Ca^{2+}$, the average and standard deviation of the distance from the Ca^{2+} to the mean plane of the C4 oxygens is 1.873 ± 0.015 Å, whereas the average distance from the metal to the mean plane of the C6 oxygens is only 1.059 ± 0.030 Å. The $(TG)(C6)Ca^{2+}$ complex is similar. For the ten lowest conformers, the average distance to the mean plane of the TG oxygens is 1.807 ± 0.048 Å, and that to the mean plane of the C6 oxygens is 1.168 ± 0.045 Å.

4. Discussion

4.1. Displacement of C4 and TG from Ca^{2+}

Measurements of ligand binding energies for alkali cations bound to dimethyl ether, dimethoxyethane, or C4 indicate that the binding energy per oxygen is greatest when the ligands are free of steric constraints and are thus able to adopt optimum binding orientations [37–41]. Thus, the energy required to remove two dimethyl ether ligands is greater than that required to remove dimethoxyethane, and the energy required to remove four dimethyl ether ligands is substantially greater than that required to remove C4, because the oxygen atoms of C4 are constrained by the crown backbone to adopt less than optimal positions around the metal center. In addition, for a given metal ion in the gas phase, the larger crowns have greater ligand binding energies than the smaller

crowns, consistent with the higher polarizabilities and greater number of donor atoms in the larger ligands. This contrasts with the "size match" correlations often observed in solution [42,43].

These principles should also apply to the complexes studied here. Like the alkali cations, alkaline earth cations form electrostatic complexes with cyclic and acyclic polyethers. Extension of these ideas to the binding of C4 and TG by Ca^{2+} suggests that C4 is almost certainly bound less strongly than TG in 1:1 complexes with Ca^{2+}, because the closed ring of C4 imposes much stronger constraints on the placement of the donor O atoms than does the backbone chain of TG. The difference in binding of the two ligands is probably even greater in the 2:1 ligand:metal complexes, where steric crowding is greater with accompanying greater constraints on the placement of the donor atoms. Further, the greater ligand binding energy arising from the larger polarizability and number of donor atoms in C6 vs. C4 provides a strong enthalpic driving force for the displacement reaction.

In light of these observations, careful examination of Table 1 reveals an apparent paradox: displacement of TG from the complexes by C6 is always more efficient than displacement of C4, even though the ligand binding energy of TG is almost certainly greater than that of C4. How can we explain this?

To rationalize the kinetic data with the expected trends in binding strengths, it is useful to take a closer look at the likely mechanism of ligand displacement. Because ligand loss is never observed in these experiments, we think it unlikely that displacement occurs via a dissociative mechanism; rather, displacement is probably an associative process that involves replacement of the donor atoms of C4 or TG by the donor atoms of an "attacking" C6 ligand.

Possible rate-limiting steps in this reaction include the rate of attachment of the C6 donors to the metal and the rate of detachment of the C4 or TG donor atoms. If C6 attachment is rate-limiting, it is expected that better "coverage" of the metal ion by the ligands initially present should result in slower rates. Because of its relative flexibility, TG should be able to cover the metal more effectively than C4. This is corroborated by the MMFF conformational search/structure calculations, which show much greater coverage of the metal by the ligands in the lowest energy conformers of the $(TG)_2Ca^{2+}$ complex than in the lowest energy conformers of $(C4)_2Ca^{2+}$ (Fig. 5). Therefore, if C6 attachment were rate limiting we would expect the reactions of TG complexes to be slower than those of the C4 complexes. This is the opposite of what is observed; as noted previously, the reactions of the TG-containing complexes are always faster than those of the analogous C4-containing species.

If the detachment of the C4 or TG donor atoms is the rate-limiting step, then (taking an Arrhenius view of the kinetics) the enthalpies and entropies of activation associated with that step will play a crucial role. As noted above, because of the greater conformational flexibility of TG, the total ligand binding enthalpy for TG bound to Ca^{2+} is almost certainly greater than that of C4, and it is also likely that the binding enthalpies for individual donor groups are greater for the O atoms of TG than for those of C4. However, it is highly unlikely that the activation barrier for ligand displacement is dependent on the total ligand binding enthalpy; rather, the barrier is probably associated with the breaking of one or more metal-donor atom bonds. It is in this key step that TG and C4 are likely to differ in such a way as to account for the faster kinetics for TG displacement. The kinetic data are consistent with a rate-limiting step that involves breaking a greater number of Ca^{2+}–O bonds for C4 than for TG. If this is the case, then both the enthalpy and entropy of activation should favor a faster reaction for TG, as observed.

The molecular dynamics calculations provide some support for the idea that more interactions are broken in the critical step for C4 displacement than in that for TG displacement. In the numerous Ca^{2+}–O dissociation events observed in the simulations of C6 attack on $(TG)_2Ca^{2+}$, essentially all were nonconcerted, as depicted in Fig. 4. A particularly interesting displacement event from the simulation is shown in more detail in Fig. 7. In this event, one of the terminal O atoms (O4) of one of the TG ligands is initially at large separation from the metal, comes into approximate binding distance (at about 3.5 ps into the simulation), then begins to move to large separation

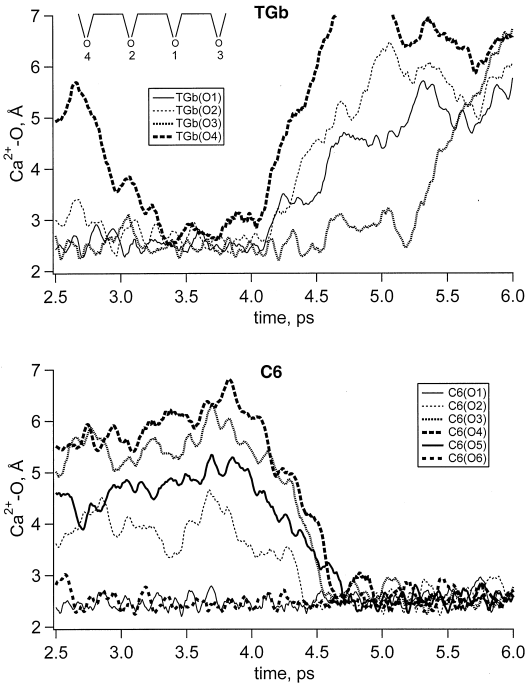

Fig. 7. Ca^{2+}–O distances during molecular dynamics simulation of displacement of TG from $(TG)_2Ca^{2+}$ by C6. Upper frame: distances to donor O atoms of one of the TG ligands (denoted ligand "TGb" in the simulation). O4 attaches, then detaches, followed by detachment of O2, O1, and O3. Lower frame: distances to donor O atoms of C6. The O atoms are numbered sequentially around the crown ring. O1 and O6 are attached to the metal throughout the simulation, O2 attaches at about 4.4 ps, followed by O3, O4, and O5.

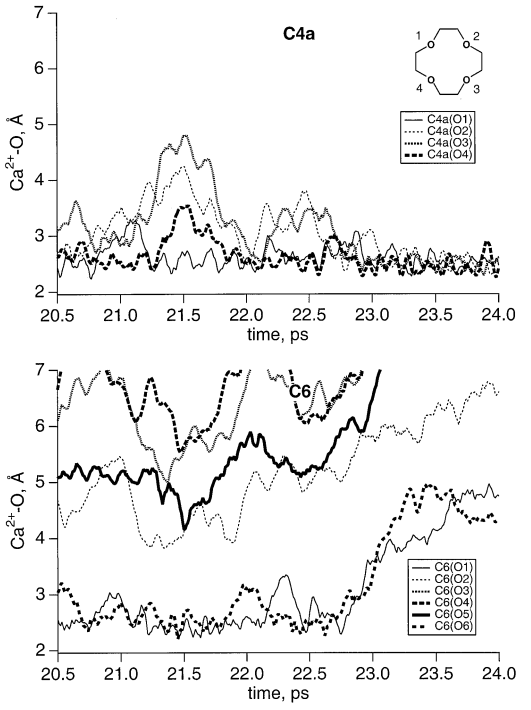

Fig. 8. Ca^{2+}–O distances during molecular dynamics simulation of displacement of C4 from $(C4)_2Ca^{2+}$ by C6. Upper frame: distances to donor O atoms of one of the C4 ligands (denoted ligand "C4a" in the simulation). Motions of O2, O3, and O4 are correlated. Lower frame: distances to donor O atoms of C6. Only O1 and O6 are attached to the metal center during the initial part of this segment of the simulation, and these two donors detach at about the same time as the C4 donors become attached.

again around the 3.75 ps mark. This is followed by the simultaneous detachment of O2 and O1 at about 4.1 ps into the simulation, whereas the last donor (O3, the other terminal oxygen) detaches more than 1 ps later. The vacancies opened in the coordination sphere of the metal are quickly occupied by donor O atoms from the attacking C6 ligand, beginning around 4.5 ps into the simulation. Thus, in accord with the scenario presented above, the displacement is initiated by association of C6 with the complex, and dissociation of the TG donor atoms one by one results in rapid replacement by the remaining C6 donors.

No exactly analogous events were observed in the simulation of C6 attack on $(C4)_2Ca^{2+}$, but a similar event is shown in Fig. 8, where C4 associates and C6 donor atoms detach. By microscopic reversibility, this is the same as a displacement of C4 by C6. Detachment of the donors from one ligand, and attachment of the donors from the other occur almost simultaneously. A key observation is that in both the events that bring C4 donor atoms to large separations from the metal center, motion of the donor atoms is correlated. For example, in the event centered on 21.5 ps simulation time, the motions of O2, O3, and O4 mirror each other, and similarly, in the event centered around 22.5 ps, O2 and O3 move together. In summary, the simulations suggest that the critical step in ligand dissociation of C4 from Ca^{2+} involves breaking two metal–ligand donor bonds in a concerted fashion.

Thus, a plausible explanation for the higher efficiency of ligand displacement for the TG complexes is that the rate-limiting step for these complexes

involves disrupting a single O–Ca^{2+} interaction, while the more rigid backbone of C4 means that the analogous rate-limiting step in C4 displacement requires disruption of two or more O–Ca^{2+} interactions. Although other explanations cannot be ruled out, this one is simple and is consistent with the molecular dynamics calculations.

Finally, we note that the second displacement, that is, displacement of C4 from (C4)(C6)Ca^{2+}, and of TG from (TG)(C6)Ca^{2+}, is especially efficient (see Table 1). Although molecular dynamics simulations of these displacements were not performed, the conformational search results suggest that at least part of the reason for the high efficiency of these reactions is that C6 dominates coordination of the metal in the mixed complexes, leaving the smaller ligand more loosely bound. For example, as noted previously, the distance from the metal to the mean plane of the C4 oxygens in $(C4)_2Ca^{2+}$ was found to be 1.589 Å, whereas in the lowest conformer of (C4)(C6)Ca^{2+} the analogous distance is 1.868 Å. Similarly, the distance from the metal to the mean plane of the TG oxygens in (TG)(C6)Ca^{2+} was calculated to be 1.864 Å. Thus, the presence of C6 in the mixed complexes weakens the interaction with the smaller ligand in such a way as to make it easier to displace.

4.2. Trends in ligand exchange kinetics with metal size

Much of the kinetics of ligand exchange can be understood on the basis of two general principles: the degree of encapsulation of the metal by ligands, and the polarizing power of the metal. The importance of metal encapsulation was recognized early in the gas phase studies of crown ether systems, and was used to explain the large differences in formation rates for 2:1 ligand:metal complexes in the reactions of the 1:1 complexes with a second ligand [44–47]. Likewise, the trends in polarizing power as the size of the metal varies have been noted with respect to their effects on reaction kinetics [47] and ligand binding strengths [17,18,37–41,48,49]. We now examine the principles of encapsulation and polarizing power in more detail, and use them to analyze the results for the alkaline earth systems studied here.

When the degree of encapsulation of the metal by the ligand dominates the reaction kinetics, metal cations with smaller radii react more slowly with incoming ligands than larger cations because the coordination shells of the smaller metals are more completely filled than those of the larger cations, blocking access by attacking ligand donor atoms. In such systems, short-range interactions between the metal ion center and the ligands must govern the kinetics, such that steric repulsions from ligands already present can prevent the close contacts necessary for effective binding with incoming ligands. Such effects are likely to be seen when at least some of the metals being compared have incompletely filled coordination shells. Because acyclic ligands such as glymes have greater conformational flexibility and therefore are better able to “cover” the metal than analogous cyclic ligands such as crown ethers, encapsulation should occur to a greater degree for a given metal in the glyme complexes than in the crown complexes. An example of a system where encapsulation is dominant is the formation of crown ether: alkali cation 2:1 complexes noted above [47], where formation reactions of the Li^+ complexes can be several orders of magnitude slower than those of larger alkali metal ions, and where reactions of the glymes are systematically slower than those of the crowns.

When polarizing power dominates the kinetics, the expected trends as metal size varies are opposite those expected for systems where encapsulation is important. As metals of a given charge decrease in size, they become increasingly better polarizers, and therefore bind ligand donor atoms more effectively. Such ideas were invoked long ago to explain the periodic trends in solvation energies as metal size varies [50]. The importance of polarizing power has been shown explicitly for the divalent alkaline earth/C6 complexes in ab initio studies [18], which found that the donor atoms of the ligand were highly polarized by the metals, and that binding strengths were greatest for the smallest alkaline earths. With deeper binding potential wells, the lifetimes of the collision com-

plexes for the smaller metals increase, with the result that unproductive dissociation back to products becomes less likely and the overall rates increase. Polarizing power is likely to be the dominant factor when all the metals being compared have completely empty or completely filled coordination shells; in other words, when the metals are either completely "bare" or are completely encapsulated, polarizing power should be the determining factor in the kinetics. Thus, we expect polarizing power to play a larger role for complexes involving acyclic ligands than for those involving cyclic ligands, because the acyclic ligands are better encapsulators and are better able to arrange the donor atoms to take advantage of the polarizing power of the metal.

The data of Table 2 and Fig. 2 can be understood in terms of these principles. Encapsulation effects primarily govern the kinetics of displacement of one ligand from $(C4)_2M^{2+}$ or $(TG)_2M^{2+}$ by C6. C4 and TG are the smallest ligands in this study, and provide the smallest degree of metal coverage, so it is reasonable to expect that the effects would be largest for these complexes. It is interesting to note that the trends as metal size varies are larger for $(C4)_2M^{2+}$ than for $(TG)_2M^{2+}$; C4 covers the metal less well than TG, so the degree of encapsulation varies more with metal size for the C4 complexes than it does for the TG complexes. In fact, the efficiencies for $(TG)_2Mg^{2+}$, $(TG)_2Ca^{2+}$, and $(TG)_2Sr^{2+}$ are all similar, suggesting that the metal is similarly well encapsulated in these three complexes; only the Ba^{2+} complex exhibits greater ligand exchange efficiency, because only in this case is encapsulation poor enough to allow facile attack by the incoming C6. Finally, it is interesting to note that the rates for a given metal are always slower for $(C4)_2M^{2+}$ than for $(TG)_2M^{2+}$, probably for the same reasons discussed in detail above for the Ca^{2+}-containing complexes: the barrier at the rate-limiting step is greater for C4 ligands than for TG, because the more rigid backbone of the crown requires disruption of a greater number of donor-metal interactions in surmounting the rate-limiting barrier.

Polarizing power plays a dominant role in the complexes containing C6 ligands, because according to x-ray data C6 is large enough to encapsulate all the alkaline earth cations [12–15,43,51]. Similarly, the conformational searches carried out on $(C4)(C6)Ca^{2+}$ and $(TG)(C6)Ca^{2+}$ (e.g. see Figure 6) found that the metal was well encapsulated in all the low-lying conformations of these complexes. Thus, in the displacements of TG from $(TG)(C6)M^{2+}$ and C4 from $(C4)(C6)M^{2+}$ by C6, the metals are encapsulated by the ligands in the complexes. Because the polarizing power of the metals decreases with increasing alkaline earth size, the collision complex well depths and rates correspondingly decrease with metal size. Again, analogous reactions for a given metal are always faster for the TG-containing systems than for the C4-containing systems, probably because the energetic cost of prying off the crown is greater than that of removing TG one donor at a time. Finally, the condensation reactions of $(C6)_2M^{2+}$ with C6 to form $(C6)_3M^{2+}$ are clearly dominated by polarizing power: all the alkaline earths in the $(C6)_2M^{2+}$ complexes are completely encapsulated, so the rates decrease monotonically with increasing metal size as the metal ions become increasingly poor polarizers and the collision complex well depths correspondingly decrease.

4.3. Trends in kinetics with ligand size

Of the ligand exchange reactions, those involving the largest ligands are most efficient, with the fastest reactions proceeding at near the collision rate. This is not surprising, because the Rice-Ramsperger-Kassel-Marcus [52,53] lifetimes of the collision complexes involving the largest ligands are longest, providing the greatest opportunity for the collision complexes to undergo exchange. The complexes of the smaller ligands, with fewer internal degrees of freedom and correspondingly shorter collision complex lifetimes, are more likely to unproductively dissociate back to reactants, and thus have lower efficiencies. The condensation reactions are slowest, because these require radiative and/or collisional stabilization, and the depth of the collision complex well is crucial, as has been pointed out for reactions involving radiative association [54]. The third ligand is undoubtedly attached weakly, so the depth of the collision complex well is

relatively shallow, collision complex lifetimes are correspondingly short, and there is a relatively high likelihood of dissociating back to reactants.

4.4. Anion effects

Host–guest stability constants measured in solution frequently depend strongly on what counterion is present. For example, log K for binding Ca^{2+} by 18-crown-6 in water changes from 0.60 ± 0.07 with Cl^- as the counterion to 1.18 ± 0.08 with NO_3^- as the counterion [43]. Of practical interest for the application of molecular recognition to solvent extraction systems, huge variations in extraction coefficients can sometimes be observed as the anion is varied. For example, extraction coefficients for tetrabutylammonium in a CH_2Cl_2/H_2O system differ by more than 10 orders of magnitude as the anion is varied from $H_2PO_4^-$ to picrate [55]. In solution, it is difficult to separate intrinsic counterion effects from contributions arising from ion pairing and ionic strength effects, so little is known about how anions influence binding intrinsically.

We have recently shown that electrospray ionization easily generates complexes of alkaline earth cations with crown ethers as doubly charged ions; as singly charged ions with a counteranion, such that the formal charge on the metal is still +2; and as singly charged ions with no counterion (formal charge of +1 on the metal) [56]. This offers unique experimental possibilities, because it makes available the two extremes in ion pairing: no ion pairing (in the case of the +2 cation) and intimate contact between cation and anion (in the case of the counterion-bearing +1 species).

Efficiencies for the displacement of C4 from $(C4)CaX^+$ ($X = CH_3COO^-$, Cl^-, Br^-, or I^-) by C6 are plotted in Fig. 9. For the halides, efficiency increases as the counteranion becomes larger and softer, perhaps reflecting a decreasing ability of the larger halides to repel the electronegative oxygens of the attacking C6 ligand. The least efficient reaction is that where acetate is the counter ion. The reasons for the decreased efficiency are not clear from the present results, but we note that acetate is considerably larger than the halides and binds the metal through a delocalized carboxylate group, perhaps providing better coverage of the metal center than a halide would in preventing close approach from the C6 donors. These preliminary results suggest ESI experiments may provide a promising avenue for the investigation of counter ion effects under simple, well-controlled conditions.

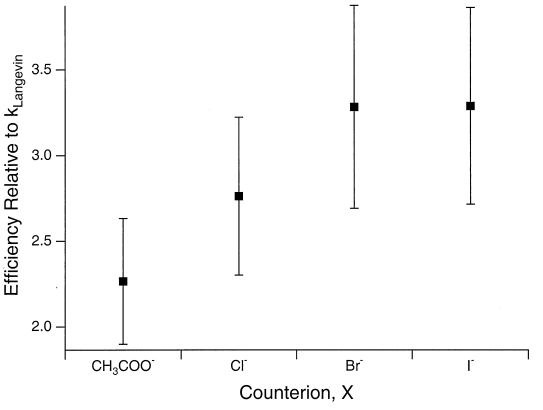

Fig. 9. Effects of varying counterion X on the efficiency of ligand displacement from $(C4)CaX^+$ by C6 ($X = CH_3COO^-$, Cl^-, Br^-, I^-). The pressure of C6 was 3.3×10^{-9} mbar. Error bars represent standard deviations from the fitting procedure used to determine rate constants and from averaging over replicate runs. The relative order of efficiencies was the same in all runs.

5. Conclusions

The seemingly complex patterns in ligand exchange reactivity for the C4, TG, C6-alkaline earth cation systems as metals and ligands are varied can be understood in terms of a few simple principles, which likely will prove to be general for complexes involving electrostatic bonding. In summary, for otherwise similar ligands reactions involving displacement of a more rigid ligand like a crown ether will tend to be slower than those involving more flexible ligands like glymes, probably because the rate-limiting step involves disruption of more metal–ligand interactions for the rigid ligand than for the flexible one. For systems where the coordination shell around the metal is partially filled, the degree to which the metal is

encapsulated by ligands is a determining factor in the rate of ligand displacement, while for systems that have no ligands or have a filled coordination shell, the polarizing power of the metal is crucial. It will be interesting to see whether or not these ideas can be usefully extended to systems that involve a greater degree of covalent metal-ligand interaction, such as transition metal-containing complexes.

Acknowledgements

The authors gratefully acknowledge support of this work by the National Science Foundation, and partial support by the donors of the Petroleum Research Fund, administered by the American Chemical Society.

References

[1] F.A. Cotton, G. Wilkinson, Advanced Inorganic Chemistry, 5th ed., Wiley, New York, 1988.
[2] P. Sadler, Adv. Inorg. Chem. 36 (1991) 1.
[3] Lectures in Bioinorganic Chemistry, P. Sadler, M. Nicolini, L. Sindellari (Eds.), Raven, New York, 1991.
[4] R.B. King, Encyclopedia of Inorganic Chemistry, Vol. 1, Wiley, New York, 1994, p. 4.
[5] N.C.J. Strynadka, M.N.G. James, Annu. Rev. Biochem. 58 (1989) 951.
[6] C.A. McPhalen, N.C.J. Strynadka, M.N.G. James, Adv. Protein Chem. 42 (1991) 77.
[7] N.C.J. Strynadka, M.N.G. James, in Calcium-Binding Proteins, R.B. King (Ed.), Encyclopedia of Inorganic Chemistry, Wiley, New York, 1994, p. 477.
[8] R.M. Izatt, R.E. Terry, B.L. Haymore, L.D. Hansen, N.K. Dalley, A.G. Avondet, J.J. Christensen, J. Am. Chem. Soc. 98 (1976) 7620.
[9] J.D. Lamb, R.M. Izatt, S.W. Swain, J.J. Christensen, J. Am. Chem. Soc. 102 (1980) 475.
[10] J.D. Lamb, R.M. Izatt, C.S. Swain, J.S. Bradshaw, J.J. Christensen, J. Am. Chem. Soc. 102 (1980) 479.
[11] H.J. Buschmann, Inorg. Chim. Acta 195 (1992) 51.
[12] N.R. Strel'tsova, L.V. Ivakina, P.A. Storozhenko, B.M. Bulyachev, V.K. Bel'skii, Dokl. Akad. Nauk. SSSR 291 (1986) 1373.
[13] V.V. Tkachev, L.O. Atovmyan, V.E. Zubareva, O.A. Raevskii, Koord. Khim. 13 (1987) 264.
[14] Y.Y. Wei, B. Tinant, J.-P. Declercq, M.V. Meerssche, J. Dale, Acta Crystallogr., Sect. C: Cryst. Struct. Commun. 44 (1988) 77.
[15] A.L. Rheingold, C.B. White, B.S. Haggerty, P. Kirlin, R.A. Gardiner, Acta Crystallogr. Sect. C 49 (1993) 808.
[16] C.W. Bauschlicher, M. Sodupe, H. Partridge, J. Chem. Phys. 96 (1992) 4453.
[17] E.D. Glendening, D. Feller, J. Phys. Chem. 100 (1996) 4790.
[18] E.D. Glendening, D. Feller, J. Am. Chem. Soc. 118 (1996) 6052.
[19] J.S. Uppal, R.H. Staley, J. Am. Chem. Soc. 104 (1982) 1229.
[20] L. Operti, E.C. Tews, B.S. Freiser, J. Am. Chem. Soc. 110 (1988) 3847.
[21] L. Operti, E.C. Tews, T.J. MacMahon, B.S. Freiser, J. Am. Chem. Soc. 111 (1989) 9152.
[22] P. Hu, M.L. Gross, J. Am. Chem. Soc. 115 (1993) 8821.
[23] H.-F. Wu, J.S. Brodbelt, J. Am. Chem. Soc. 116 (1994) 6418.
[24] G. Siuzdak, Y. Ichikawa, T.J. Caulfield, B. Munoz, C.-H. Wong, K.C. Nicolaou, J. Am. Chem. Soc. 115 (1993) 2877.
[25] L. Chen, A.G. Marshall, Int. J. Mass Spectrom. Ion Processes 79 (1987) 115.
[26] L. Chen, T.-C.L. Wang, T.L. Ricca, A.G. Marshall, Anal. Chem. 59 (1987) 449.
[27] J.E. Bartmess, R.M. Georgiadis, Vacuum 33 (1983) 149.
[28] K.J. Miller, J.A. Savchik, J. Am. Chem. Soc. 101 (1979) 7206.
[29] K.J. Miller, J. Am. Chem. Soc. 112 (1990) 8533.
[30] L.R. Anders, J.L. Beauchamp, R.C. Dunbar, J.D. Baldeschwieler, J. Chem. Phys. 45 (1966) 1062.
[31] S.J. Weiner, P.A. Kollman, D.T. Nguyen, D.A. Case, J. Comput. Chem. 7 (1986) 230.
[32] Q. Chen, K. Cannell, J. Nicoll, D.V. Dearden, J. Am. Chem. Soc. 118 (1996) 6335.
[33] T.A. Halgren, J. Comput. Chem. 17 (1996) 490.
[34] G. Gioumousis, D.P. Stevenson, J. Chem. Phys. 29 (1958) 294.
[35] T. Su, M.T. Bowers, in Classical Ion–Molecule Collision Theory, M.T. Bowers (Ed.), Gas Phase Ion Chemistry Vol. 1, Academic, New York, 1979, p. 83.
[36] T. Su, M.T. Bowers, J. Chem. Phys. 58 (1973) 3027.
[37] D. Ray, D. Feller, M.B. More, E.D. Glendening, P.B. Armentrout, J. Phys. Chem. 100 (1996) 16116.
[38] M.B. More, D. Ray, P.B. Armentrout, J. Phys. Chem. A 101 (1997) 831.
[39] M.B. More, D. Ray, P.B. Armentrout, J. Phys. Chem. A 101 (1997) 7007.
[40] M.B. More, D. Ray, P.B. Armentrout, J. Phys. Chem. A 101 (1997) 4254.
[41] M.B. More, D. Ray, P.B. Armentrout, J. Am. Chem. Soc. 121 (1999) 417.
[42] R.M. Izatt, J.H. Rytting, D.P. Nelson, B.L. Haymore, J.J. Christensen, Science 164 (1969) 443.
[43] R.M. Izatt, K. Pawlak, J.S. Bradshaw, R.L. Bruening, Chem. Rev. 91 (1991) 1721.
[44] H. Zhang, I.-H. Chu, S. Leming, D.V. Dearden, J. Am. Chem. Soc. 113 (1991) 7415.
[45] H. Zhang, D.V. Dearden, J. Am. Chem. Soc. 114 (1992) 2754.
[46] D.V. Dearden, H. Zhang, I.-H. Chu, P. Wong, Q. Chen, Pure Appl. Chem. 65 (1993) 423.
[47] I.H. Chu, H. Zhang, D.V. Dearden, J. Am. Chem. Soc. 115 (1993) 5736.
[48] M.B. More, E.D. Glendening, D. Ray, D. Feller, P.B. Armentrout, J. Phys. Chem. 100 (1996) 1605.
[49] D. Walter, M.R. Sievers, P.B. Armentrout, Int. J. Mass Spectrom. Ion Processes 175 (1998) 93.
[50] M. Born, Z. Phys. 1 (1920) 15.

[51] R.D. Shannon, Acta Crystallogr., Sect. A: Found. Crystallogr. 32 (1976) 751.
[52] R.A. Marcus, O.K. Rice, J. Phys. Colloid Chem. 55 (1951) 894.
[53] R.A. Marcus, J. Chem. Phys. 20 (1952) 359.
[54] V. Ryzhov, R.C. Dunbar, Int. J. Mass Spectrom. Ion Processes 167 (1997) 627.
[55] F. Montanari, S. Quici, S. Banfi, in Phase Transfer Catalysis, D.N. Reinhoudt (Ed.), Supramolecular Technology Vol. 10, Elsevier, Oxford, 1996, p. 389.
[56] R.M. Pope, N. Shen, J. Nicoll, B. Tarnawiecki, C. Dejsupa, D.V. Dearden, Int. J. Mass Spectrom. Ion Processes 162 (1997) 107.